

This discussion paper is/has been under review for the journal Atmospheric Chemistry and Physics (ACP). Please refer to the corresponding final paper in ACP if available.

**Synergetic use of  
millimeter and  
centimeter  
wavelength radars**

S. Y. Matrosov

# Synergetic use of millimeter and centimeter wavelength radars for retrievals of cloud and rainfall parameters

**S. Y. Matrosov**

Cooperative Institute for Research in Environmental Sciences, University of Colorado and NOAA/Earth System Research Laboratory, Boulder, CO, USA

Received: 14 December 2009 – Accepted: 28 December 2009 – Published: 18 January 2010

Correspondence to: S. Y. Matrosov (sergey.matrosov@noaa.gov)

Published by Copernicus Publications on behalf of the European Geosciences Union.

Title Page

Abstract

Introduction

Conclusions

References

Tables

Figures

⏪

⏩

◀

▶

Back

Close

Full Screen / Esc

Printer-friendly Version

Interactive Discussion

## Abstract

A remote sensing approach for simultaneous retrievals of cloud and rainfall parameters in the vertical column above the US Department of Energy's (DOE) Climate Research Facility at the Tropical Western Pacific (TWP) Darwin site in Australia is described. This approach uses vertically pointing measurements from a DOE  $K_a$ -band radar and scanning measurements from a nearby C-band radar pointing toward the TWP Darwin site. Rainfall retrieval constraints are provided by data from a surface impact disdrometer. The approach is applicable to stratiform precipitating cloud systems when a separation between the liquid hydrometeor layer, which contains rainfall and liquid water clouds, and the ice hydrometeor layer is provided by the radar bright band. Absolute C-band reflectivities and  $K_a$ -band vertical reflectivity gradients in the liquid layer are used for retrievals of the mean layer rain rate and cloud liquid water path (CLWP). C-band radar reflectivities are also used to estimate ice water path (IWP) in regions above the melting layer. The retrieval uncertainties of CLWP and IWP for typical stratiform precipitation systems are about  $500\text{--}800\text{ g m}^{-2}$  (for CLWP) and a factor of 2 (for IWP). The CLWP retrieval uncertainties increase with rain rate, so retrievals for higher rain rates may be impractical. The expected uncertainties of layer mean rain rate retrievals are around 20%, which, in part, is due to constraints available from the disdrometer data. The applicability of the suggested approach is illustrated for two characteristic events observed at the TWP Darwin site during the wet season of 2007. A future deployment of W-band radars at the DOE tropical Climate Research Facilities can improve CLWP estimate accuracies and provide retrievals for a wider range of stratiform precipitating cloud events.

## 1 Introduction

Discriminating between small drop cloud liquid water, which is suspended in the atmosphere, and precipitating liquid water contained in larger raindrops is a challenging

## Synergetic use of millimeter and centimeter wavelength radars

S. Y. Matrosov

Title Page

Abstract

Introduction

Conclusions

References

Tables

Figures

⏪

⏩

◀

▶

Back

Close

Full Screen / Esc

Printer-friendly Version

Interactive Discussion

remote sensing problem. Liquid water clouds and rain often coexist in the same atmospheric layer (e.g., Dubrovina, 1982; Mazin, 1989), which makes their separation difficult. Estimates of the suspended and precipitating water are essential for cloud and climate model verification purposes, so a comprehensive characterization of hydrometeors (including liquid water and ice) in the vertical atmospheric column is one of the important objectives of the Atmospheric Radiation Measurement (ARM) Program (Ackerman and Stokes, 2003), which was recently incorporated into US Department of Energy's (DOE) Atmospheric System Research (ASR) program.

A novel radar-based remote sensing method was recently suggested for simultaneous retrievals of cloud liquid water path (CLWP), a layer-mean rainfall rate,  $R_m$ , or rain water path (RWP), and cloud ice water path (IWP) in the vertical atmospheric column above the ARM Southern Great Plains (SGP) Central Facility (Matrosov, 2009a, b). This method uses measurements from the ground-based vertically pointing DOE  $K_a$ -band Millimeter-wavelength Cloud Radar (MMCR) and the W-band Cloud radar (WACR) which operate at wavelengths of 8.7 and 3.2 mm, correspondingly. The retrievals of parameters in the liquid hydrometeor layer are based on estimates of attenuation of cloud radar signals in this layer, and estimates of IWP are based on absolute MMCR reflectivity measurements corrected for attenuation in the liquid and melting layers (and also for attenuation by the wet radome) using observations from a scanning S-band Weather Surveillance Radar-1988 Doppler (WSR-88D), which has an identifier KVN<sub>X</sub> and is located at a distance of about 60 km from the SGP site. Rain drop size distribution (DSD) measurements from a ground-based Joss-Waldvogel (1967) disdrometer (JWD), which is collocated with the DOE radars, are used to constrain retrievals. JWD data are corrected for the "dead" time effects according to Sheppard and Joe (1994).

The suggested SGP remote sensing method is applicable to stratiform precipitating systems which exhibit radar melting layer signatures (e.g., the reflectivity bright band – BB); thus the vertical separation of the liquid hydrometeor layer containing liquid water clouds and rain from the cloud regions, which contain predominantly ice, is readily avail-

---

**Synergetic use of millimeter and centimeter wavelength radars**S. Y. Matrosov

---

Title Page

Abstract

Introduction

Conclusions

References

Tables

Figures

⏪

⏩

◀

▶

Back

Close

Full Screen / Esc

Printer-friendly Version

Interactive Discussion

able. The attenuation-based retrievals in the liquid hydrometeor layer provide estimates of layer integrated (e.g., CLWP) or layer mean values (e.g.,  $R_m$ ). The vertical variability of non-attenuated cloud radar reflectivities in the rain layer is not known for SGP measurements and it is a contributor to the retrieval uncertainty, which is accounted for when estimating retrieval errors. Although this variability in stratiform precipitation is generally small (e.g., Bellon et al., 2005) and usually amounts to only 1–1.5 dB (or even less at W-band due to strong non-Rayleigh scattering effects; Matrosov, 2007), accounting for it directly in retrievals will make them more robust.

Estimating the variability of non-attenuated reflectivity in rain requires vertical profiles of radar observations at frequencies where attenuation is negligible (e.g., S- or C-bands). These observations should be collocated with the profiles of attenuated ARM cloud radar measurements, so the effects of cloud radar signal attenuation can be better separated from the effects of vertical variability of non-attenuated reflectivities. The KVN radar measurements cannot be used for S-band vertical profiles estimates in the rain layer above the DOE SGP site because of the scanning strategy employed by the weather service radars and also due to a poor cross-beam resolution, which is  $\sim 1$  km at a 60 km range.

At the Tropical Western Pacific (TWP) Darwin DOE site, however, the availability of high resolution C-band reflectivity profiles over the MMCR radar from the nearby scanning polarimetric radar (C-POL) provides a means for accounting for the vertical variability of non-attenuated reflectivities. While this site lacks a W-band radar, a combination of C-band and  $K_a$ -band radar measurements still can be used for retrieving parameters of precipitating clouds (although at the expense of increased CLWP retrieval uncertainties).

## 2 An approach to retrieve cloud and rain parameters from MMCR and C-POL

Although a future deployment of W- and X-band radars is planned for the TWP Darwin site, the MMCR and C-POL measurements are currently the only routinely available

### Synergetic use of millimeter and centimeter wavelength radars

S. Y. Matrosov

Title Page

Abstract

Introduction

Conclusions

References

Tables

Figures

⏪

⏩

◀

▶

Back

Close

Full Screen / Esc

Printer-friendly Version

Interactive Discussion



## Synergetic use of millimeter and centimeter wavelength radars

S. Y. Matrosov

Title Page

Abstract

Introduction

Conclusions

References

Tables

Figures

◀

▶

◀

▶

Back

Close

Full Screen / Esc

Printer-friendly Version

Interactive Discussion

radar data at this site. The MMCR, located at the DOE TWP facility, provides vertically pointing measurements (Moran et al., 1998), and the scanning C-POL radar (Keenan et al., 1998), located at a 25.5 km distance from this facility, regularly (once in 10 min) performs the range-height indicator (RHI) scans over the MMCR. These RHI scans are used to reconstruct the vertical profiles of C-band radar reflectivity, so two frequency reflectivity profiles (i.e., at  $K_a$ - and C-bands) are available over the TWP Darwin site. The availability of the JWD deployed near the MMCR at this site since 2007 allows constraining rain rate retrievals.

The total two-way attenuation of MMCR signals (in decibels),  $\Delta Z_K$ , in the liquid hydrometeor layer between the lowest unsaturated MMCR range gate and the bottom of the melting layer is caused by rain, liquid water clouds and atmospheric gases and it can be given as

$$\Delta Z_K = 2C_K R_m \Delta h + 2B_K \text{CLWP} + G_K, \quad (1)$$

where  $\Delta h$  is a thickness of this layer and  $G_K$  is the two-way gaseous absorption, which is calculated assuming a 90% relative humidity in the liquid hydrometeor precipitation layer. The attenuation  $\Delta Z_K$  linearly depends on CLWP because cloud droplets, which are generally smaller than 50  $\mu\text{m}$ , are within the Rayleigh scattering regime for radar wavelengths, so there is a linear relation between cloud liquid water content and the attenuation coefficient. The linearity of the  $K_a$ -band attenuation coefficient in rain as a function of rain rate is due to the proportionality of both these quantities to the similar moments of rain DSDs (e.g., Matrosov et al., 2006). The expressions for the coefficients  $C_K$  and  $B_K$  are given by Matrosov (2009a).

The mean rain rate  $R_m$  is calculated as

$$R_m = \Delta h^{-1} \int_{h_0}^{h_m} R(h) dh \quad (2)$$

where the integration is carried out from the height of the lowest unsaturated MMCR range gate ( $h_0$ ) to the height of the base of the melting layer ( $h_m$ ), and  $\Delta h = h_m - h_0$ . The

vertical profile of rain rate,  $R(h)$ , is estimated based on the profiles of C-POL reflectivities,  $Z_{ec}(h)$ , and the  $Z_{ec}-R$  relations, which are established for each observational case based on the data from the JWD

$$R(h) = (1/a)^{(1/b)} Z_{ec}(h)^{(1/b)}. \quad (3)$$

5 The  $Z_{ec}-R$  relations are expressed in the power law form

$$Z_{ec} = a R^b, \quad (4)$$

where the equivalent radar reflectivity at C-band  $Z_{ec}$  is in  $\text{mm}^6 \text{m}^{-3}$  and  $R$  is in  $\text{mm h}^{-1}$ .

It is assumed that the JWD estimates of rain rate,  $R_{\text{JWD}}$ , are representative for the rainfall at the lowest height  $h_0$ , so

$$10 R_{\text{JWD}} = R(h_0) = (1/a)^{(1/b)} Z_{ec}(h_0)^{(1/b)}. \quad (5)$$

The reported C-POL radar reflectivity profile is then corrected so that the observed shape of the profile is retained but it is shifted by a constant value of  $\Delta Z$  in such a way that the resulting reflectivity value at the height  $h_0$  would correspond to the value  $Z_{ec}(h_0)$  as calculated from  $R_{\text{JWD}}$ ,  $a$  and  $b$  using Eq. (5). As a result, a consistency of  
 15 C-POL estimates of rain rate is achieved by constraining them with the surface-based estimates of  $R$  (i.e.,  $R_{\text{JWD}}$ ), which are considered as “ground truth”. In other words, the observed vertical profile of C-POL estimates describes the vertical changes of rain rate in the liquid hydrometeor layer using Eq. (3) where values of  $Z_{ec}$  represent the reported C-POL values corrected by  $\Delta Z$ . The  $\Delta Z$  correction accounts for any miscalibrations and not-accounted losses of C-POL signals, which could originally exist. Since the MMCR vertical gate spacing ( $\sim 90 \text{m}$ ) is finer than that of C-POL RHI estimates above the MMCR site ( $\sim 300 \text{m}$ ), the linear interpolation is used to recalculate C-POL reflectivities to the MMCR vertical resolution points.

25 After the layer mean rain rate,  $R_m$ , is estimated from Eqs. (2) and (3), where the corrected (i.e., shifted by the value of  $\Delta Z$ ) C-POL reflectivity profile is used, the CLWP value in the liquid hydrometeor layer between  $h_0$  and  $h_m$  is calculated using Eq. (1). In

**Synergetic use of millimeter and centimeter wavelength radars**

S. Y. Matrosov

Title Page

Abstract

Introduction

Conclusions

References

Tables

Figures



Back

Close

Full Screen / Esc

Printer-friendly Version

Interactive Discussion



---

**Synergetic use of  
millimeter and  
centimeter  
wavelength radars**


---

S. Y. Matrosov

[Title Page](#)
[Abstract](#)
[Introduction](#)
[Conclusions](#)
[References](#)
[Tables](#)
[Figures](#)




[Back](#)
[Close](#)
[Full Screen / Esc](#)
[Printer-friendly Version](#)
[Interactive Discussion](#)


Eq. (1), the  $K_a$ -band reflectivity difference due to attenuation (i.e.,  $\Delta Z_K$ ) is estimated by subtracting reflectivity difference due to the change of non-attenuated reflectivity between heights  $h_m$  and  $h_0$ , (i.e.,  $\Delta Z_{KC}$ ), from the MMCR observed reflectivity difference between these heights (i.e.,  $\Delta Z_{KO}$ ), so it becomes

$$CLWP = 0.5(\Delta Z_{KO} - \Delta Z_{KC} - 2C_K R_m \Delta h - G_K) B_K^{-1} \quad (6)$$

The C-POL reflectivity difference between heights  $h_m$  and  $h_0$  is used as a proxy for the value of  $\Delta Z_{KC}$ . This is justified by the fact that differences between non-attenuated reflectivities in stratiform rainfall at C- and  $K_a$ -bands are usually very small (as shown in the next section). Attenuation of C-band signals in rain is much smaller than that of  $K_a$ -band signals and it is accounted for using differential phase shift measurements (note that differential phase based corrections of C-POL reflectivities for attenuation in intervening rain areas between the C-POL radar and the TWP Darwin site were generally less than 1 dB for experimental examples considered in Sect. 3). Moreover, due to the slant low elevation angle viewing geometry of the C-POL radar measurements, this C-band attenuation is expected to be very similar for C-POL signals at all the heights in the liquid layer above the MMCR. Because of that, the difference in the reported C-band reflectivities at the bottom and at the top of the liquid hydrometeor layer is an appropriate substitute for the difference in non-attenuated reflectivities at the boundaries of this layer.

In the SGP stratiform precipitating cloud retrieval approach (Matrosov, 2009a), estimates of the ice water content (IWC) and its vertical integral – ice water path (IWP) are based on the MMCR reflectivity data which are attenuation corrected above the melting level height using KVN<sub>X</sub> measurements. The IWC- $Z_e$  relations are used for these estimates. For the TWP Darwin site, C-POL measurements above this height are more appropriate for this purpose. There are several reasons for that. First, unlike the KVN<sub>X</sub> radar, which provides only a few data points over the SGP MMCR, the C-POL radar provides relatively high resolution vertical profiles of reflectivity above the TWP Darwin MMCR. In addition to that, the TWP MMCR is less sensitive than the SGP MMCR, and the total attenuation in the liquid layer is generally larger for similar rainfalls at the

TWP site (compared to the SGP site) because melting layers are generally higher in tropics. As a result, some significant parts of precipitating systems above the melting layer could be missed by the TWP MMCR (as will be shown in Fig. 1).

### 3 Examples of simultaneous cloud and rain retrievals at the TWP Darwin site

In spite of a tropical location of the TWP Darwin site and the occurrence of strong convection during the monsoon season, stratiform rainfall is also common there. Two characteristic events from the wet season of 2007 are described below.

#### 3.1 Observational data

Two examples of the stratiform precipitating events observed at the TWP Darwin site on 27 January 2007 and 27 February 2007 are shown in Fig. 1. The time-height cross sections of reflectivities at  $K_a$ -band (as measured by the vertically pointing MMCR in the general operational mode) and C-band (as reconstructed from the C-POL RHI scans, which are performed every 10 min) are depicted. The reflectivity enhancements in the melting layer (i.e., the bright band – BB), which separates the liquid hydrometeor layer and the layer where the ice phase dominates, are clearly seen at both frequency bands. It can be also seen that the C-POL radar echo tops are higher than those from the MMCR, which is due to the high attenuation of  $K_a$ -band signals by the liquid and melting hydrometeors and also by the wet radome. Note that the general MMCR mode is its the most robust mode, and although it has an unambiguous Doppler velocity threshold of only about  $5 \text{ m s}^{-1}$ , the reflectivity estimates account for velocity aliasing in rain measurements when Doppler velocities exceed the unambiguous velocity value.

The markedly different vertical structures of  $K_a$ - and C-band reflectivities are obvious from Fig. 1. While reflectivity values from vertically pointing MMCR measurements in the liquid hydrometeor layer below BB exhibit very pronounced diminishing trend with height as a result of attenuation by rain and liquid water clouds, C-band reflectivity pro-

## Synergetic use of millimeter and centimeter wavelength radars

S. Y. Matrosov

Title Page

Abstract

Introduction

Conclusions

References

Tables

Figures

⏪

⏩

◀

▶

Back

Close

Full Screen / Esc

Printer-friendly Version

Interactive Discussion

---

**Synergetic use of  
millimeter and  
centimeter  
wavelength radars**S. Y. Matrosov

---

[Title Page](#)[Abstract](#)[Introduction](#)[Conclusions](#)[References](#)[Tables](#)[Figures](#)[⏪](#)[⏩](#)[◀](#)[▶](#)[Back](#)[Close](#)[Full Screen / Esc](#)[Printer-friendly Version](#)[Interactive Discussion](#)

files in this layer change in the vertical rather insignificantly. Figure 2 illustrates this fact by showing examples of MMCR and C-POL reflectivity profiles for two different times for both experimental cases from Fig. 1. The steeper vertical gradients in MMCR reflectivity correspond to higher rain rates and larger C-band reflectivities. The BB reflectivity enhancement is sharper in the MMCR data due to their finer vertical resolution. To avoid a BB contamination of liquid layer reflectivity measurements, a relatively conservative value of the melting layer bottom height  $h_m=4$  km was chosen for retrievals. A value of 0.3 km was chosen for  $h_0$  because examining the data indicates that at lower heights, MMCR measurements are sometimes saturated and C-POL measurements might have some beam blockage problems. The significant difference in MMCR and C-POL reflectivities at the lowest “good” gate (i.e., at the  $h_0$  height), where attenuation due to hydrometeors is expected to be very small, can be explained by the attenuation caused by the wet MMCR radome. This fact does not cause problems, because the MMCR reflectivity differences and not their absolute values are used for retrievals.

The low variability of C-POL measurements in the rain layer is expected for stratiform precipitation. Figure 3 depicts time series of the mean and the standard deviation (SD) of the C-POL reflectivities in a vertical profile between heights of  $h_m$  and  $h_0$ . It can be seen that SD values usually vary between 1 and 2 dB and are, on average about 1.5 dB. This is in general agreement with the results of Bellon et al. (2005) and Matrosov et al. (2007) who indicated a low vertical variability of longer wavelength reflectivity in stratiform rainfall. SD values are practically independent of the profile mean reflectivities, which vary quite significantly (e.g., between about 20 and 38 dBZ for the event of 27 February 2007).

Figure 4 shows rainfall accumulations obtained by time integrating of  $R_{JWD}$  values inferred from JWD DSDs. The JWD-based accumulation estimates are in very good agreement with the collocated 0.01” resolution tipping bucket rain gauge values, which are also depicted. Such gauges are the standard meteorological instruments used for rainfall accumulation measurements, so the observed agreement provides confidence in JWD rain rate data used to constrain retrievals. For the event of 27 January 2007,

rain rates varied modestly and the accumulation increased at a relatively steady rate. For the 27 February 2007 event, two periods of heavier rain were observed between 11:30 and 12:30 UTC and between 16:00 and 17:00 UTC.

As mentioned above, the  $Z_{ec}-R$  relations and C-POL measurements are used to estimate mean layer rain rate,  $R_m$ . These relations are established for each observational case. Figure 6 shows the  $Z_{ec}-R$  scatter plots calculated from the JWD DSD measurements during the stratiform rain events considered in this study. It can be seen from this figure that while there is some event-to-event variability in the coefficients of these relations (i.e.,  $Z_{ec}=411R^{1.41}$  for 27 January 2007 vs.  $Z_{ec}=237R^{1.34}$  for 27 February 2007), overall the data scatter within individual events is not very significant. The relative standard deviation of the data points with respect to the best fit power-law approximations is about 20% and 25% for the events of 27 January 2007 and 27 February 2007, correspondingly.

Since measurements of C-POL reflectivity near the boundaries of the liquid hydrometeor layer (i.e.,  $h_m$  and  $h_0$ ) are used to estimate the contribution of changes in non-attenuated MMCR reflectivity  $\Delta Z_{KC}$  to the total change of the MMCR reflectivity in this layer, it is important to evaluate the validity of using C-band reflectivity differences as a proxy for  $K_a$ -band reflectivity differences. JWD data allow such evaluations. Figure 6 shows a scatter plot of C- and  $K_a$ -band radar reflectivities as calculated from JWD DSDs observed during the event of 27 February 2007. The data from the event of 27 January 2007 are similar and not shown. The T-matrix approach (Barber and Yeh, 1975) and non-spherical rain drop shape (Brandes et al., 2005) were used for calculating C-POL and MMCR radar reflectivities from experimental DSDs.

Frequency dependences of non-Rayleigh scattering effects and refractive indices of water can result in discrepancies between C- and  $K_a$ -band rainfall reflectivities. These discrepancies, however, in typical stratiform rains are usually less than about 1 dB (Fig. 6). Furthermore, for simultaneous C-POL and MMCR vertical profiles, the discrepancies between non-attenuated reflectivity differences at these two frequency bands [i.e.,  $Z_{ec}(h_0)-Z_{ec}(h_m)$  which is  $\Delta Z_{KC}$ , and  $Z_{ek}(h_0)-Z_{ek}(h_m)$ ] are expected to be,

## Synergetic use of millimeter and centimeter wavelength radars

S. Y. Matrosov

Title Page

Abstract

Introduction

Conclusions

References

Tables

Figures

◀

▶

◀

▶

Back

Close

Full Screen / Esc

Printer-friendly Version

Interactive Discussion

on average, even smaller than such discrepancies for single reflectivity values. This is because the non-attenuated reflectivities vary little in the vertical in stratiform rains, so the magnitudes non-Rayleigh scattering effects, which generally increase with reflectivity, are expected to be similar at different heights in the vertical profile. As a result a partial cancelation of these effects will take place for the reflectivity differences. This justifies using C-POL measurements to estimate vertical changes of non-attenuated MMCR reflectivities. Reflectivity measurement noise can also contribute to the uncertainty of estimating reflectivity differences between the boundaries of the liquid hydrometeor layer. To mitigate this factor, three point mean values of C-POL reflectivities in the vicinity of both  $h_m$  and  $h_0$  rather than single point reflectivities at these heights were used to estimate vertical changes of non-attenuated reflectivities in the liquid hydrometeor layer.

### 3.2 Results of cloud and rainfall parameter retrievals

Figure 7 presents the time series of simultaneous retrievals of the mean layer rain rate  $R_m$ , IWP and CLWP of precipitating cloud systems shown in Fig. 1. IWP values correspond to cloud regions located above the melting level, and CLWP and  $R_m$  represent the liquid hydrometeor layer. Ice/snow particles above the melting layer in stratiform events generally dominate radar backscatter (e.g., Shupe et al. 2004), so reflectivity measurements can be used to estimate ice content. Since C-band measurements are used in accounting for the shape of the vertical profiles of  $K_a$ -band non-attenuated reflectivities and C-POL RHI scans over the MMCR are performed only once in every 10 min, retrievals are carried out only at the times of C-POL RHI scans. Thus there are generally only 6 retrieval points per hour. The MMCR and JWD data used for the retrievals are averaged in the  $\pm 0.5$  min intervals centered at the times of the RHI scans.

During the event of 27 January 2007 (Fig. 7a), the mean layer rain rates generally varied in a range between 2 and 6 mm h<sup>-1</sup>, which is rather typical for stratiform rainfall. The variability in retrieved CLWP is more significant. The CLWP values generally varied in a range between 0 and 3000 g m<sup>-2</sup>. Occasional CLWP retrieval points were slightly

## Synergetic use of millimeter and centimeter wavelength radars

S. Y. Matrosov

Title Page

Abstract

Introduction

Conclusions

References

Tables

Figures

◀

▶

◀

▶

Back

Close

Full Screen / Esc

Printer-friendly Version

Interactive Discussion



## Synergetic use of millimeter and centimeter wavelength radars

S. Y. Matrosov

Title Page

Abstract

Introduction

Conclusions

References

Tables

Figures

⏪

⏩

◀

▶

Back

Close

Full Screen / Esc

Printer-friendly Version

Interactive Discussion

negative (e.g., around 10:00 UTC). The occurrence of such unrealistic negative estimates is (as will be shown in the next section) a consequence of high CLWP retrieval uncertainties. The IWP values are noticeably greater than those of CLWP and reach  $8000 \text{ g m}^{-2}$ . As mentioned in Sect. 2, IWP was calculated by vertically integrating the IWC values estimated from the C-POL reflectivity measurements. The relation  $\text{IWC} (\text{g m}^{-3}) = 0.04 Z_{\text{ec}}^{0.6} (\text{mm}^6 \text{ m}^{-3})$  was used for ice content estimates. This relation was obtained with in situ microphysical data set used for deriving mm-wavelength IWC- $Z_e$  relations for high reflectivity ice clouds as described by Matrosov and Heymsfield (2008).

The columnar cloud and rainfall parameters during the 27 February 2007 event (Fig. 7b) were more variable than those for the event of 27 January 2007. Although the average rain rate for this February event ( $\sim 2.5 \text{ mm h}^{-1}$ ) was lower than that for the January event ( $\sim 3.3 \text{ mm h}^{-1}$ ), there were two periods (around 12:00 and 16:30 UTC in Fig. 7b) with more significant rainfall. The second of these periods was accompanied also by increases in cloud CLWP and IWP. The CLWP values exhibited higher variability but overall they were similar to those retrieved for the 27 January 2007 case. Due to generally lower C-POL cloud top heights and weaker reflectivities above the melting layer for the February event (Fig. 1b vs. Fig. 1d), the retrieved IWP values in Fig. 7b are on average significantly smaller compared to those in Fig. 7a. It should be mentioned that the lowest reflectivities measured by the C-POL radar near the cloud tops are about  $-5$ – $-10 \text{ dBZ}$ . While due to sensitivity limitations, this radar might not detect cloud parts with lower reflectivities (thus not observing “true” cloud tops), this fact should not significantly bias the IWP retrievals because usually more than 90% of the ice cloud mass in stratiform precipitating systems comes from cloud parts with reflectivities that are greater than  $0 \text{ dBZ}$  (e.g., Matrosov and Heymsfield 2008).

Columnar characteristics of rainfall can also be given in terms of rain water path (RWP) instead of the mean layer rain rate,  $R_m$ , because there is a relatively tight relation between rain water content (RWC) and  $R$ . Figure 8 shows the RWC- $R$  relations as calculated from the JWD DSDs. It can be seen that these relations are close to

linear and the difference between best fit approximations for the experimental events considered here is relatively small. Since C-POL measurements are used to provide the vertical structure of rain rates (with the JWD constraint as discussed above), RWC profiles can also be estimated using relations presented in Fig. 8. The RWP values can be then calculated by vertically integrating RWC. Time series of the RWP estimates for the precipitating systems considered in this study are shown in Fig. 9. The mean layer rain rates are also shown for a reference.

#### 4 Assessment of retrieval uncertainties

Under the described retrieval approach for the TWP Darwin site, the simultaneous estimates of hydrometeor parameters in precipitating systems are performed independently in the liquid hydrometeor layer (for  $R_m$  and CLWP) and in the ice regions above the melting level (for IWP). Estimates of the mean layer rain rate,  $R_m$ , are based on the C-POL reflectivity measurements using case specific  $Z_{ec}-R$  relations and constrained by the JWD data. As shown above, the individual data scatter around the case specific  $Z_{ec}-R$  relations is relatively low ( $\sim 20-25\%$ ). When estimating the mean layer rain rate by integrating profiles of  $R$  using Eq. (2), some partial cancelation of individual point errors in a rainfall profile can be expected, so a 20% uncertainty in inferring the  $R_m$  value could be reasonable. An uncertainty in estimating RWP is expected to be similar to that of  $R_m$ , due to the relatively tight RWC- $R$  relations.

While retrievals of  $R_m$  are independent of cloud liquid since small cloud drops contribute negligibly to radar backscatter in presence of rain, estimates of CLWP for a given vertical column, which are based on attenuation effects and are performed using Eq. (6), depend on  $R_m$  estimates in the same vertical column. Two main sources of the CLWP retrieval uncertainty are the measurement error in the observed reflectivity difference  $\Delta Z_{KO}-\Delta Z_{KC}$ , and the uncertainty in the two-way rainfall attenuation term  $2C_K R_m \Delta h$ . The CLWP uncertainty  $\delta(\text{CLWP})$  due to the first of these two sources can

### Synergetic use of millimeter and centimeter wavelength radars

S. Y. Matrosov

Title Page

Abstract

Introduction

Conclusions

References

Tables

Figures

⏪

⏩

◀

▶

Back

Close

Full Screen / Esc

Printer-friendly Version

Interactive Discussion

be given as

$$\delta(\text{CLWP})_1 = \delta Z (2B_K)^{-1} \quad (7)$$

where  $\delta Z$  is the error in the reflectivity difference measurements. The second main uncertainty source results in

$$\delta(\text{CLWP})_2 = \delta R_m C_K \Delta h / B_K^{-1}. \quad (8)$$

The coefficients  $B_K$  and  $C_K$ , which describe specific  $K_a$ -band attenuation in liquid water clouds and rain do not significantly depend on DSD details and are about  $0.87 \text{ dB km}^{-1} \text{ g}^{-1} \text{ m}^3$  and  $0.26 \text{ dB km}^{-1} \text{ mm}^{-1} \text{ h}$ , correspondingly (e.g., Matrosov et al., 2006). While the temperature dependence of  $C_K$  is negligible,  $B_K$  exhibits some relatively modest temperature variability. It was assumed during retrievals that the mean liquid cloud temperature was equal to the mean temperature in the liquid hydrometeor layer, which was known from the radiozonde soundings.

Figure 10 shows the estimated retrieval error  $\delta(\text{CLWP})$  suggesting the independence of these two main error contributions (i.e.,  $\delta(\text{CLWP})^2 = \delta(\text{CLWP})_1^2 + \delta(\text{CLWP})_2^2$ ) and assuming an uncertainty for the reflectivity difference estimates  $\delta Z = 1 \text{ dB}$ . The two error terms considered above are responsible for the bulk of the CLWP retrieval uncertainty. The gaseous attenuation term  $G_K$  due water vapor and oxygen is relatively small at  $K_a$ -band (Stepanenko et al., 1987). The model uncertainties of this term calculations are expected not to exceed few tenths of 1 dB and here the corresponding uncertainty is considered to be absorbed by the uncertainty in the reflectivity difference estimates  $\delta Z$ . The influence of temperature uncertainties in  $B_K$  on the retrieval errors is minor compared to the two main uncertainty sources considered above (Matrosov, 2009a).

It can be seen from Fig. 10 that the CLWP error is generally quite high and it increases with the mean layer rain rate as attenuation by rain in the liquid hydrometeor layer gradually overwhelms attenuation by liquid clouds as  $R_m$  increases. For a typical TWP stratiform event of 27 January 2007, when  $R_m$  values generally varied between about 2 and  $6 \text{ mm h}^{-1}$ , LWP retrieval uncertainties can be in a range of 600–1000  $\text{g m}^{-2}$ . Such relatively large uncertainties mean that retrievals of lower values of

**Synergetic use of millimeter and centimeter wavelength radars**

S. Y. Matrosov

Title Page

Abstract

Introduction

Conclusions

References

Tables

Figures

⏪

⏩

◀

▶

Back

Close

Full Screen / Esc

Printer-friendly Version

Interactive Discussion



CLWP with the radars that are currently available at the TWP Darwin site might be not reliable. It also explains the fact that CLWP retrievals can occasionally provide unrealistic negative estimates and exhibit significant fluctuations.

For heavier rainfall which was occasionally observed during the event of 27 February 2007 (e.g.,  $R_m \sim 8\text{--}14 \text{ mm h}^{-1}$ ), LWP uncertainties can be very high reaching 2000–2500  $\text{g m}^{-2}$  which could make cloud liquid water path retrievals impractical. Such large CLWP retrieval errors are, in part, due to high altitude of the melting layer ( $\Delta h$ ) which is usually observed in the tropics. Attenuation due to rain is proportional to  $\Delta h$  resulting in higher values of  $\delta(\text{CLWP})_2$  according to Eq. (8). Another reason of high CLWP retrieval uncertainties at the TWP Darwin site is that the  $K_a$ -band MMCR signals are relatively weakly attenuated by liquid water clouds. At W-band frequencies, attenuation in liquid water clouds is about a factor of 5 stronger than that at  $K_a$ -band while attenuation ratio in rain for these two frequency bands is only about a factor of 3 (Matrosov, 2009a). As a result, the relative contribution of cloud attenuation to the total attenuation by liquid hydrometeors at W-band is greater by approximately 60–70%.

Additional advantages of W-band radars over  $K_a$ -band radars for the purpose of attenuation-based CLWP and rain retrievals are in much larger observed reflectivity differences due to attenuation and lower vertical variability of non-attenuated reflectivities due to stronger non-Rayleigh scattering effects at higher radar frequencies. While there are some disadvantages too (e.g., more data scatter in the rain attenuation – rain rate relations at W-band compared to  $K_a$ -band), overall, the future use of vertically-pointing ground-based W-band radars (when available) instead (or in addition) of the  $K_a$ -band MMCR will improve the retrievals of CLWP in stratiform precipitating systems observed at the TWP Darwin site.

In the suggested approach, the IWP values are obtained by vertically integrating IWC profiles estimated from CPOL reflectivities, so the IWP retrieval errors are determined by those of IWC. The IWC estimate errors mostly come from the uncertainties in the IWC- $Z_e$  relations. Generally about a factor of 2 uncertainty in the radar reflectivity based estimates of IWC can be expected (e.g., Protat et al., 2007) due to the data

---

## Synergetic use of millimeter and centimeter wavelength radars

S. Y. Matrosov

---

Title Page

Abstract

Introduction

Conclusions

References

Tables

Figures

⏪

⏩

◀

▶

Back

Close

Full Screen / Esc

Printer-friendly Version

Interactive Discussion

scatter in the individual IWC- $Z_e$  points used to derive best fit power law reflectivity – ice content relations. While accounting for temperature can improve accuracies of radar-based estimates of ice content for smaller values of IWC, for larger ice contents, which are common for precipitating cloud systems, the temperature information might not be of significant help for ice content estimates (e.g., Matrosov and Heymsfield, 2008). It is assumed in this study that a factor of 2 uncertainty is also representative for IWP estimates, although some opposite sign error cancelation might occur when vertically integrating IWC values.

## 5 Conclusions

Measurements from the vertically pointing  $K_a$ -band MMCR radar at the TWP Darwin ARM Climate Research Facility (ACRF), the reflectivity profiles over this facility from the nearby CPOL C-band scanning polarimetric radar and surface disdrometer data can be used for estimations of cloud and rainfall parameters in stratiform precipitation events. CPOL data constrained by the disdrometer measurements provide estimates of the mean rain rate,  $R_m$ , and/or RWP in the liquid hydrometeor layer located between the surface and the melting layer, which boundaries are clearly identifiable from radar data. The attenuation-based approach utilizing the MMCR data provides estimates of CLWP for clouds, which co-exist with rain in the liquid hydrometeor layer but are not detectable against the rain background in the absolute reflectivity measurements. The availability of C-band vertical reflectivity profiles over the ACRF site improves the attenuation-based CLWP estimates by allowing separation of the effects of  $K_a$ -band signal attenuation from effects of the vertical changes of non-attenuated reflectivity in this layer. The CPOL profiles are also used for retrieving IWP values (and/or IWC profiles) over the ACRF site above the melting layer so the characterization of liquid and ice hydrometeors and a separation of suspended (i.e. cloud) and precipitating (i.e., rainfall) liquid in a vertical column over this site becomes possible.

The near surface rain rate constraint from disdrometer measurements, which are, in

## Synergetic use of millimeter and centimeter wavelength radars

S. Y. Matrosov

Title Page

Abstract

Introduction

Conclusions

References

Tables

Figures

⏪

⏩

◀

▶

Back

Close

Full Screen / Esc

Printer-friendly Version

Interactive Discussion



---

**Synergetic use of  
millimeter and  
centimeter  
wavelength radars**S. Y. Matrosov

---

Title Page

Abstract

Introduction

Conclusions

References

Tables

Figures

⏪

⏩

◀

▶

Back

Close

Full Screen / Esc

Printer-friendly Version

Interactive Discussion

turn, validated by the gauge measurements and the availability of the vertical profiles of C-band reflectivity help to reduce uncertainties of mean layer rain rate retrievals. These uncertainties are estimated at about 20%. Expected uncertainties of CLWP retrievals are significantly more substantial. These uncertainties are estimated as about 500–800 g m<sup>2</sup> for lower rain rates up to about 4 mm h<sup>-1</sup> and they increase with  $R_m$ , as attenuation of K<sub>a</sub>-band radar signals in rain becomes progressively more dominant compared to attenuation by liquid water clouds. Such large CLWP uncertainties may result in the “retrieval noise” and can make liquid cloud parameter retrievals for events with lower CLWP and higher rain rates impractical with currently available instruments. Uncertainties of the IWP retrievals are expected to be about a factor of 2, which is rather common for the reflectivity-based estimates of cloud ice content.

The application of the suggested remote sensing approach devised for the TWP Darwin ACRF was illustrated using two stratiform rainfall events observed during the wet period of 2007. The thickness of the liquid hydrometeor layer during these events was around 4 km. Mean layer rain rates for these events were typically between 2 and 4 mm<sup>-1</sup>, although periods of heavier rainfall were observed. The retrievals indicated IWP changes in an approximate range between 10<sup>3</sup> and 10<sup>4</sup> g m<sup>2</sup>. Average CLWP values were approximately 1000–1500 g m<sup>2</sup>. Retrievals of lower CLWP values (less than ~500–800 g m<sup>2</sup>) could be compromised by high uncertainties.

The high CLWP retrieval uncertainties are, in part, due to relatively low attenuation rate of MMCR K<sub>a</sub>-band signals by liquid water clouds. The future plans for the DOE TWP ACRFs include deployments of W-band radars which signals are attenuated by liquid phase significantly stronger compared to MMCR signals. Besides, the ratio of attenuations by liquid clouds and by rain (for given water amounts) is larger at W-band compared to K<sub>a</sub>-band. The aforementioned factors and the lower variability of non-attenuated reflectivities at higher radar frequencies are expected to improve retrieval accuracies of CLWP when W-band radars are used. A further improvement is likely to come when vertically pointing cm-wavelength radar or profiler measurements (e.g., at X-band or S-band) will be added. This addition will allow higher vertical resolution esti-

mates of non-attenuated reflectivity and a better collocation of mm- and cm-wavelength radar measurements in the vertical column. It will also significantly improve temporal resolution of retrievals, which are now available only for the times of the C-POL RHI scans.

- 5 *Acknowledgement.* This research was supported by the Office of Science (BER), US Department of Energy, Grant No. DE-FG02-05ER63954. The author thanks M. Whippey, P. May and A. Protat from the Centre for Australian Weather and Climate Research for providing C-POL data.

## References

- 10 Ackerman, T. P. and Stokes, G.: The atmospheric radiation measurement program, *Phys. Today*, 56, 38–45, 2003.
- Barber, P. and Yeh, C.: Scattering of electromagnetic waves by arbitrarily shaped dielectric bodies, *Appl. Optics*, 14, 2864–2872, 1975.
- Brandes, E. A., Zhang, G., and Vivekanandan, J.: Corrigendum, *J. Appl. Meteorol.*, 43, 1541–1553, 2005.
- 15 Bellon, A., Lee, G. W., and Zawadzki, I.: Error statistics in VPR corrections in stratiform precipitation, *J. Appl. Meteorol.*, 44, 998–1015, 2005.
- Dubrovina, L. S.: Cloudness and precipitation according to the data of airplane soundings, *Gidrometeoizdat, Leningrad*, 218 pp., 1982 (in Russian).
- 20 Joss, J. and Waldvogel, A.: Ein Spektrograph für Niederschlagstropfen mit automatischer Auswertung, *Pure Appl. Geophys.*, 68, 240–246, 1967.
- Keenan, T. D., Glasson, K., Cummings, F., Bird, T. S., Keeler, J., and Lutz, J.: The BMRC/NCAR C-band polarimetric (C-POL) radar system, *J. Atmos. Ocean. Tech.*, 15, 871–886, 1998.
- Matrosov, S. Y., May, P. T., and Shupe, M. D.: Rainfall profiling using atmospheric radiation measurement program vertically pointing 8-mm wavelength radars, *J. Atmos. Ocean. Tech.*, 23, 1478–1491, 2006.
- 25 Matrosov, S. Y.: Potential for attenuation-based estimations of rainfall rate from CloudSat, *Geophys. Res. Lett.*, 34, L05817, doi:10.1029/2006GL029161, 2007.
- Matrosov, S. Y., Clark, C. A., and Kingsmill, D. A.: A polarimetric radar approach to identify rain,

## Synergetic use of millimeter and centimeter wavelength radars

S. Y. Matrosov

Title Page

Abstract

Introduction

Conclusions

References

Tables

Figures

⏪

⏩

◀

▶

Back

Close

Full Screen / Esc

Printer-friendly Version

Interactive Discussion



melting-layer, and snow regions for applying corrections to vertical profiles of reflectivity, *J. Appl. Meteorol. Clim.*, 46, 154–166, 2007.

Matrosov, S. Y. and Heymsfield, A. J.: Estimating ice content and extinction in precipitating cloud systems from CloudSat radar measurements. *J. Geophys. Res.*, 113, D00A05, doi:10.1029/2007JD009633, 2008.

Matrosov, S. Y.: A method to estimate vertically integrated amounts of cloud ice and liquid and mean rate in stratiform precipitation from radar and auxiliary data, *J. Appl. Meteorol. Clim.*, 48, 1398–1410, 2009a.

Matrosov, S. Y.: Simultaneous estimates of cloud and rainfall parameters in the atmospheric vertical column above the ARM Southern Great Plains site, *J. Geophys. Res.*, 114, D22201, doi:10.1029/2009JD012004, 2009b.

Mazin, I. P.: *Clouds and the Cloudy Atmosphere*, Gidrometeoizdat, Leningrad, 648 pp., 1989.

Moran, K. P., Marttner, B. E., Post, M. J., Kropfli, R. A., Welsh, D. C., and Widener, K. B.: An unattended cloud-profiling radar for use in climate research, *B. Am. Meteorol. Soc.*, 79, 443–455, 1998.

Protat, A., Delanoe, J., Bouniol, D., Heymsfield, A. J., Bansemir, A., and Brown, P.: Evaluation of ice water content retrievals from cloud radar reflectivity and temperature using a larger airborne in situ microphysical database, *J. Appl. Meteorol. Clim.*, 46, 557–572, 2007.

Sheppard, B. E. and Joe, P. I.: Comparisons of raindrop size distribution measurements by a Joss-Waldvogel disdrometer, a PMS 2DG spectrometer, and a POSS Doppler radar, *J. Atmos. Ocean. Tech.*, 11, 874–887, 1994.

Shupe, M. D., Kollias, P., Matrosov, S. Y., and Schneider, T. L.: Deriving mixed-phase cloud properties from Doppler radar spectra, *J. Atmos. Ocean. Tech.*, 21, 660–670, 2004.

Stepanenko, V. D., Schukin, G. G., Bobylev, L. P., and Matrosov, S. Y.: *Microwave Radiometry in Meteorology*, Gidrometeoizdat, Leningrad, 284 pp., 1987.

**Synergetic use of millimeter and centimeter wavelength radars**

S. Y. Matrosov

Title Page

Abstract

Introduction

Conclusions

References

Tables

Figures

⏪

⏩

◀

▶

Back

Close

Full Screen / Esc

Printer-friendly Version

Interactive Discussion

## Synergetic use of millimeter and centimeter wavelength radars

S. Y. Matrosov

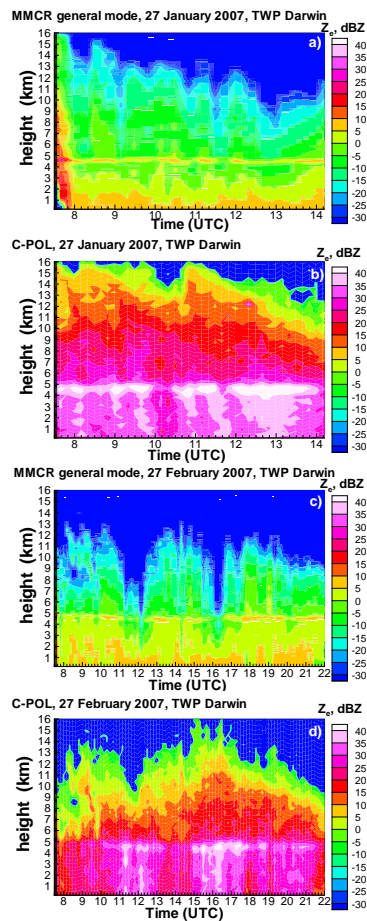


**Fig. 1.** TWP Darwin MMCR (a and c) and C-POL (b and d) reflectivity cross sections observed in stratiform precipitation events on 22 January 2007 (a and b) and 22 February 2007 (a and b).

Title Page

Abstract

Introduction

Conclusions

References

Tables

Figures

◀

▶

◀

▶

Back

Close

Full Screen / Esc

Printer-friendly Version

Interactive Discussion

Synergetic use of  
millimeter and  
centimeter  
wavelength radars

S. Y. Matrosov

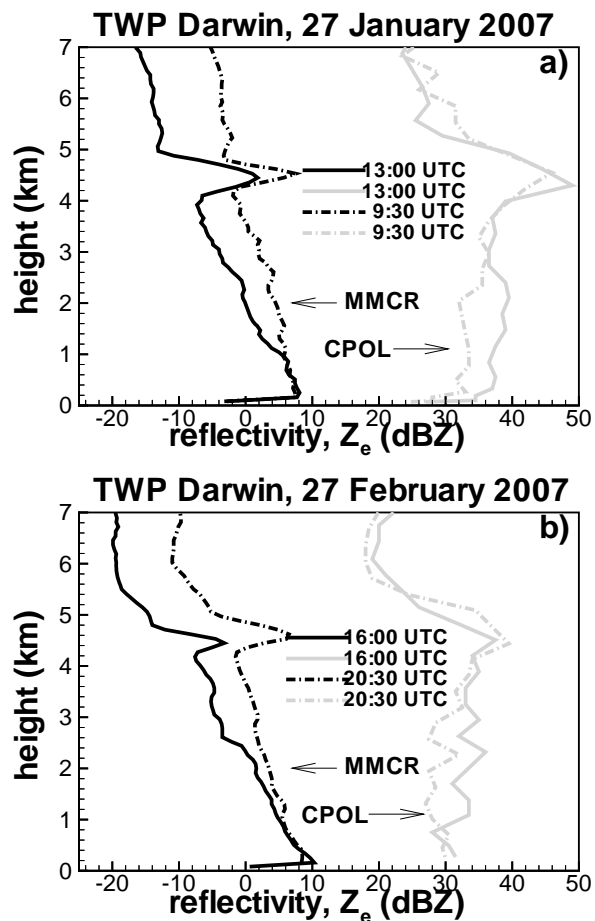


**Fig. 2.** Vertical profiles of MMCR and C-POL reflectivity observed at two different times during the stratiform precipitating events of 27 January 2007 (a) and 27 February 2007 (b).

[Title Page](#)[Abstract](#)[Introduction](#)[Conclusions](#)[References](#)[Tables](#)[Figures](#)[◀](#)[▶](#)[◀](#)[▶](#)[Back](#)[Close](#)[Full Screen / Esc](#)[Printer-friendly Version](#)[Interactive Discussion](#)

**Synergetic use of  
millimeter and  
centimeter  
wavelength radars**

S. Y. Matrosov

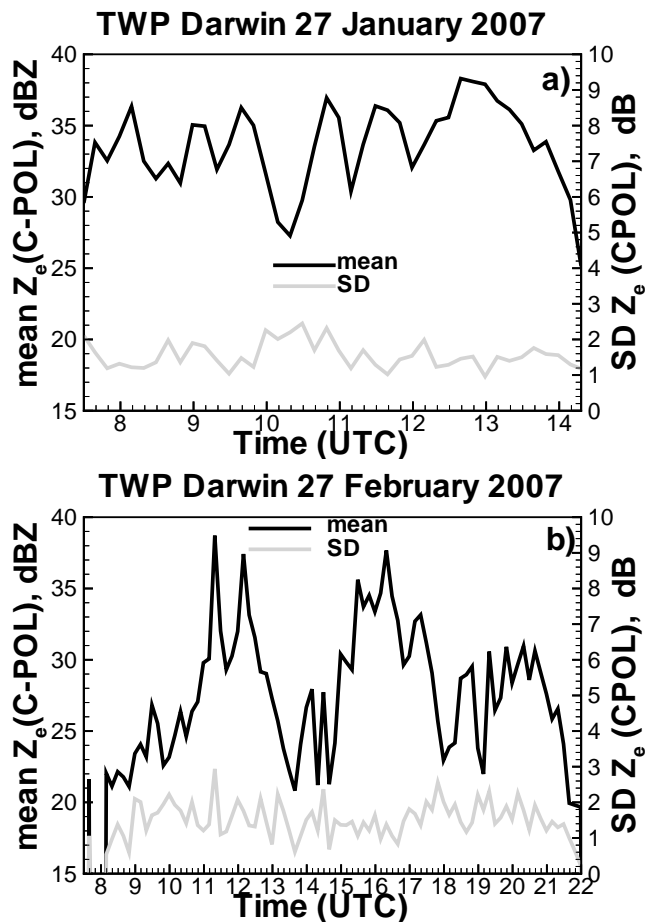


**Fig. 3.** Time series of mean and standard deviation values of C-POL reflectivity vertical profiles in the rain layer for the events of 27 January 2007 (a) and 27 February 2007 (b).

[Title Page](#)[Abstract](#)[Introduction](#)[Conclusions](#)[References](#)[Tables](#)[Figures](#)[◀](#)[▶](#)[◀](#)[▶](#)[Back](#)[Close](#)[Full Screen / Esc](#)[Printer-friendly Version](#)[Interactive Discussion](#)

## Synergetic use of millimeter and centimeter wavelength radars

S. Y. Matrosov

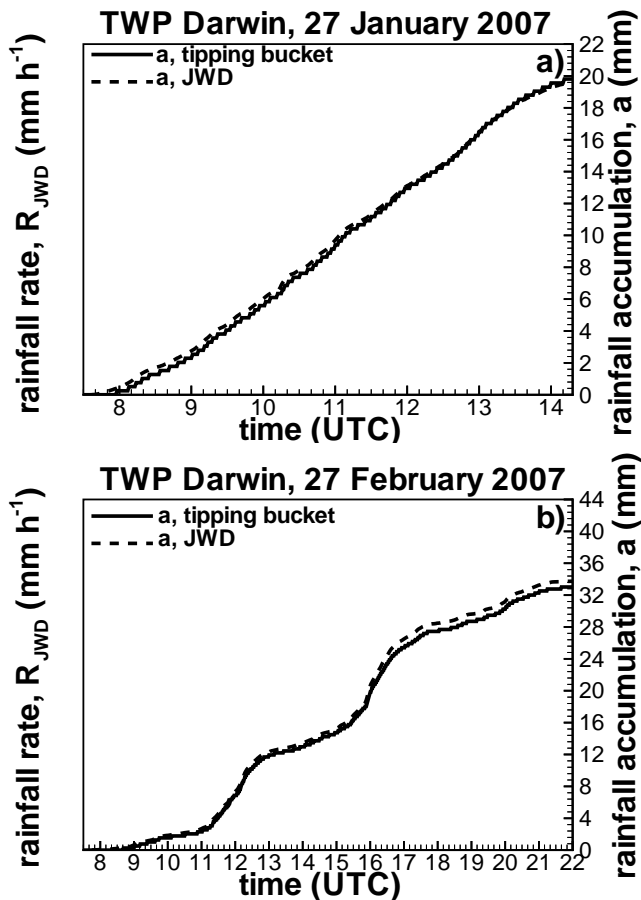


**Fig. 4.** Time series of rainfall accumulation from the JWD and rain gauge at the TWP Darwin site for the events of 27 January 2007 (a) and 27 February 2007 (b).

[Title Page](#)[Abstract](#)[Introduction](#)[Conclusions](#)[References](#)[Tables](#)[Figures](#)[◀](#)[▶](#)[◀](#)[▶](#)[Back](#)[Close](#)[Full Screen / Esc](#)[Printer-friendly Version](#)[Interactive Discussion](#)

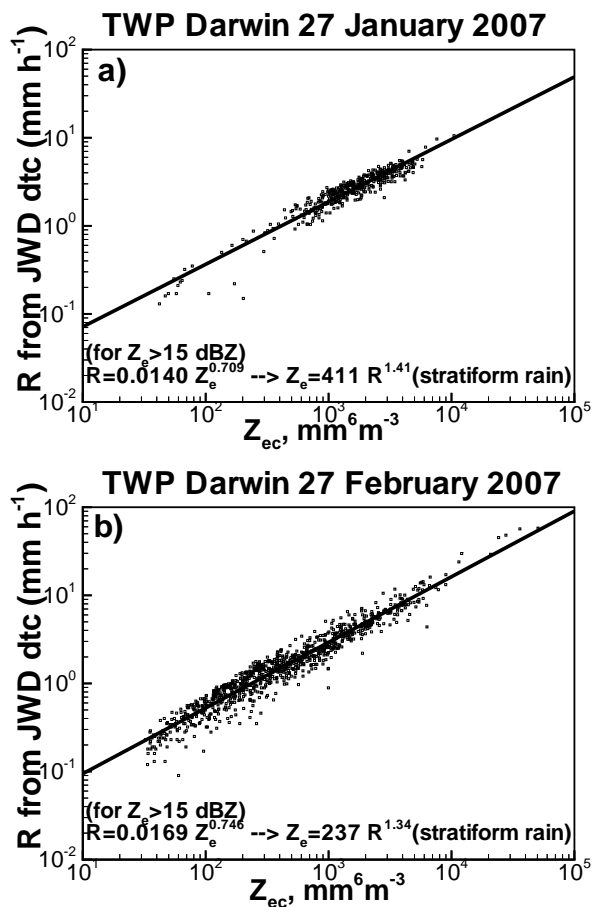


**Fig. 5.** Scatter plots of C-band radar reflectivity and versus rain rate as calculated from the JWD DSDs measured during the events of 27 January 2007 **(a)** and 27 February 2007 **(b)**.

[Title Page](#)
[Abstract](#)
[Introduction](#)
[Conclusions](#)
[References](#)
[Tables](#)
[Figures](#)
[⏪](#)
[⏩](#)
[◀](#)
[▶](#)
[Back](#)
[Close](#)
[Full Screen / Esc](#)
[Printer-friendly Version](#)
[Interactive Discussion](#)

**Synergetic use of  
millimeter and  
centimeter  
wavelength radars**

S. Y. Matrosov

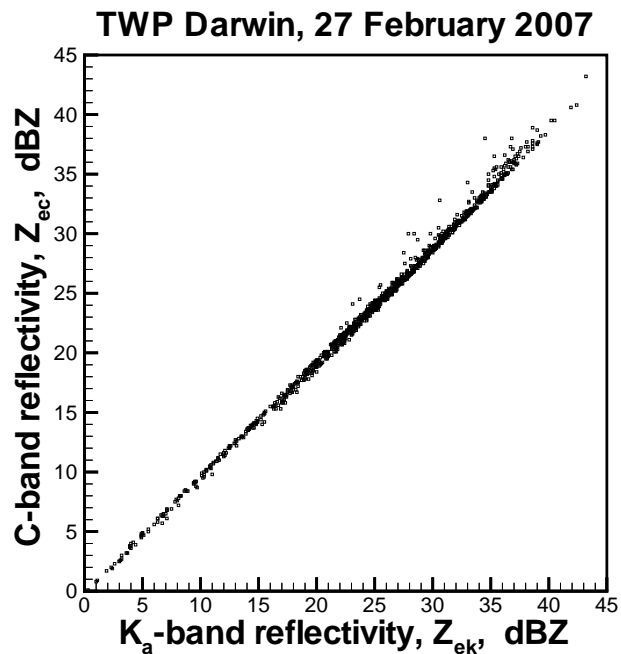


**Fig. 6.** Scatter plot of C-POL reflectivities versus MMCR reflectivities as calculated from the JWD DSDs.

[Title Page](#)[Abstract](#)[Introduction](#)[Conclusions](#)[References](#)[Tables](#)[Figures](#)[◀](#)[▶](#)[◀](#)[▶](#)[Back](#)[Close](#)[Full Screen / Esc](#)[Printer-friendly Version](#)[Interactive Discussion](#)

Synergetic use of  
millimeter and  
centimeter  
wavelength radars

S. Y. Matrosov

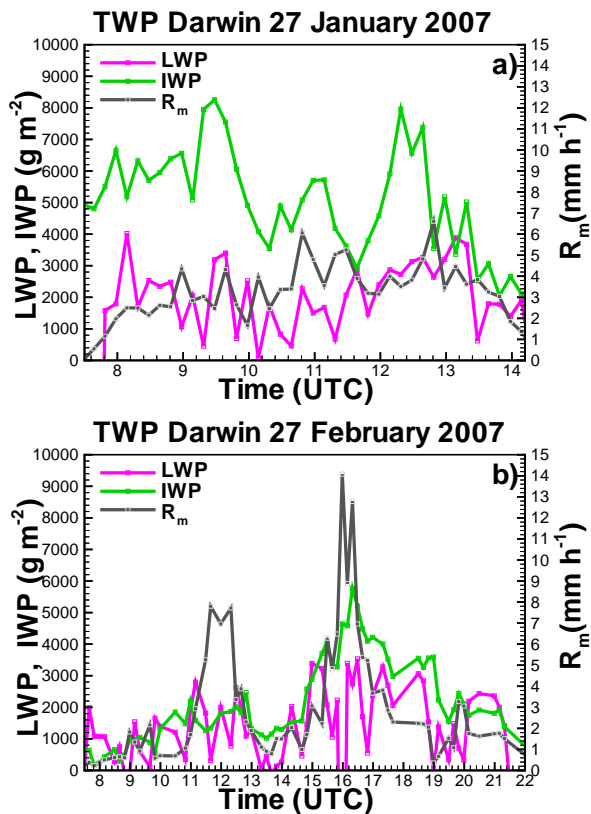


**Fig. 7.** Retrievals of cloud LWP, IWP and mean layer rain rate in the vertical column above the ARM TWP Darwin site during the 27 January 2007 (a) and 27 February 2007 (b) stratiform precipitating events.

[Title Page](#)[Abstract](#)[Introduction](#)[Conclusions](#)[References](#)[Tables](#)[Figures](#)[◀](#)[▶](#)[◀](#)[▶](#)[Back](#)[Close](#)[Full Screen / Esc](#)[Printer-friendly Version](#)[Interactive Discussion](#)

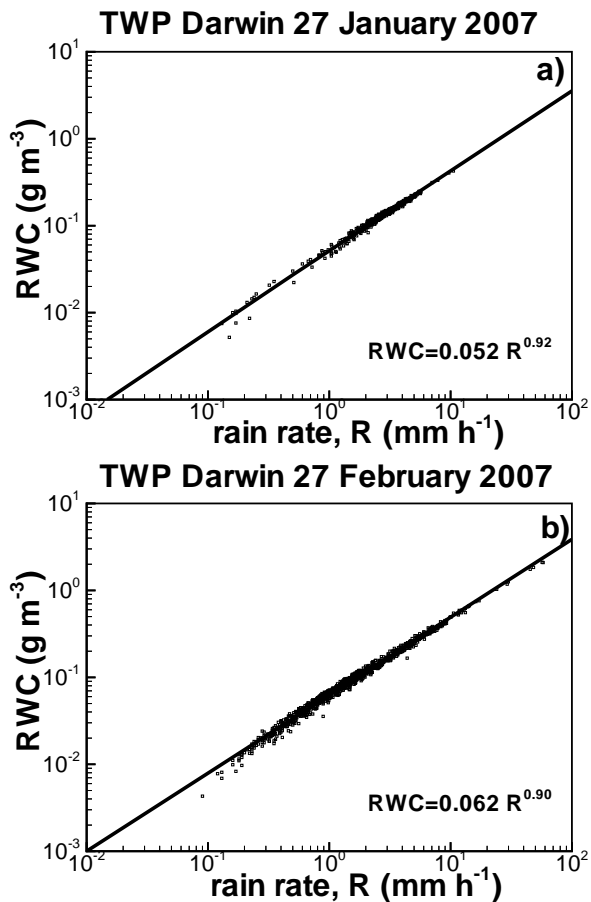


**Fig. 8.** Scatter plots of rain water content versus rain rate as calculated from JWD DSDs for the events of 27 January 2007 (a) and 27 February 2007 (b).

[Title Page](#)[Abstract](#)[Introduction](#)[Conclusions](#)[References](#)[Tables](#)[Figures](#)[◀](#)[▶](#)[◀](#)[▶](#)[Back](#)[Close](#)[Full Screen / Esc](#)[Printer-friendly Version](#)[Interactive Discussion](#)

Synergetic use of  
millimeter and  
centimeter  
wavelength radars

S. Y. Matrosov

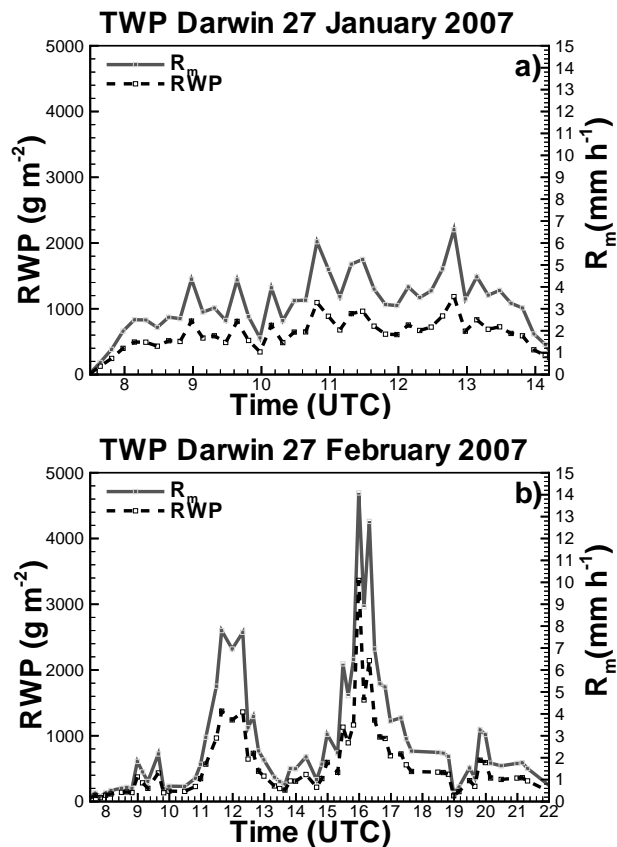


**Fig. 9.** Retrievals RWP and mean layer rain rate during the 27 January 2007 **(a)** and 27 February 2007 **(b)** stratiform precipitating events.

[Title Page](#)[Abstract](#)[Introduction](#)[Conclusions](#)[References](#)[Tables](#)[Figures](#)[⏪](#)[⏩](#)[◀](#)[▶](#)[Back](#)[Close](#)[Full Screen / Esc](#)[Printer-friendly Version](#)[Interactive Discussion](#)

**Synergetic use of  
millimeter and  
centimeter  
wavelength radars**

S. Y. Matrosov

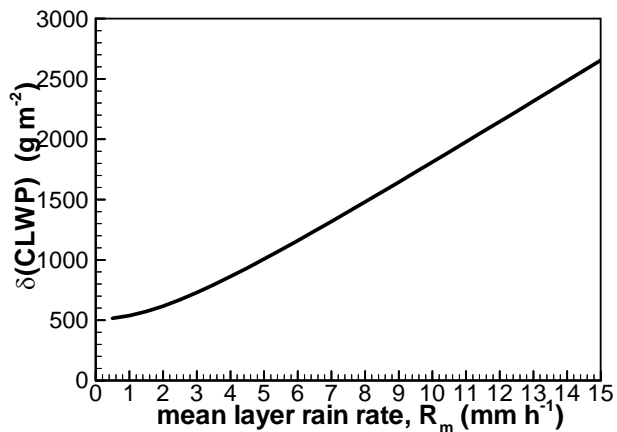


**Fig. 10.** Estimates of the LWP retrieval error as a function of the mean layer rain rate.

[Title Page](#)[Abstract](#)[Introduction](#)[Conclusions](#)[References](#)[Tables](#)[Figures](#)[⏪](#)[⏩](#)[◀](#)[▶](#)[Back](#)[Close](#)[Full Screen / Esc](#)[Printer-friendly Version](#)[Interactive Discussion](#)